Interdisciplinary Information Sciences, Vol. 1, No. 2, pp. 121–132 (1995)

Numerical Study on Wave Propagation in a Branched Lattice of LC Circuit

Kazufumi OZAWA*, Masami OKADA** and Hiromi KOKUTA**

**Education Center for Information Processing, Tohoku University, Kawauchi, Aoba-ku, Sendai 980-77, Japan, and*
***Graduate School of Information Sciences, Tohoku University, Katahira, Aoba-ku, Sendai 980-77, Japan*

Received March 9, 1994; final version accepted October 11, 1994

Linear and nonlinear wave propagations of soliton-like pulse waves are studied by solving the second order ordinary differential equations numerically. The model in which the wave propagations are considered is the one-dimensional infinite lattice of an LC (inductor-capacitor) circuit with a branching point. The behaviors of the soliton-like pulse waves before and after passing through the branching point are observed in detail. These observations show that after passing through the point the original waves are split into two, reflected and transmitted, for both the linear and nonlinear cases. Although, in general, the behaviors of these two waves are very complex and difficult to analyze, a theoretical analysis using the continuous approximation to the model is possible in some cases.

KEYWORDS: branched lattice, lattice soliton, nonlinear LC circuit, numerical analysis, localized mode

1. Introduction

The theory of the one-dimensional nonlinear (i.e. exponential) lattice has been extensively developed since the 1960's (see for example [11], [14]). In this note, we present some numerical results on the linear and nonlinear wave propagations in a branched LC lattice circuits since it seems to the present authors that neither experimental nor numerical work on the wave propagation in the lattice has ever been appeared. The aim of this paper is to study in detail the phenomenon of the transmission and the reflection of pulse waves at a branching point.

First of all, we introduce the branched infinite LC circuit in order to obtain our system of equations. The picture is depicted as in Figure 1, where V_n is the signal voltage across the n-th capacitor C and I_n is the electric current through the n-th coil with a linear (constant) inductance L. Let Q_n be the stored charge in the n-th capacitor.

We shall consider two cases. The first is the linear case where $Q_n = V_n$, and the second is the nonlinear (exponential) case where $Q_n = \log(1 + V_n)$. When the lattice has no branch, the former case is a classical electric circuit (low pass filter), and the latter case was studied in [4] as a model of the well-known Toda lattice (anharmonic lattice with exponential interaction) in the corresponding nonlinear mechanical system [11], [12]. In the following, the values of C and L are assumed to be 1 for simplicity. Then the circuit equations of this LC network are given by

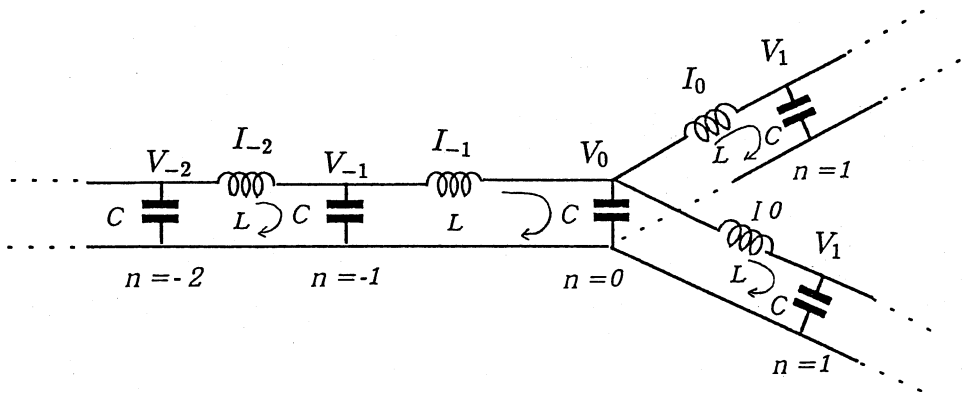

Fig. 1

This work is partially supported by a Grant-in-Aid for Scientific Research (No. 05640145), Ministry of Education, Science and Culture.

$$\begin{cases} \dot{Q}_n(t) = I_{n-1}(t) - I_n(t), \\ \dot{I}_n(t) = V_n(t) - V_{n+1}(t), \quad (n \neq 0), \end{cases} \tag{1}$$

$$\begin{cases} \dot{Q}_0(t) = I_{-1}(t) - 2I_0(t), \\ \dot{I}_0(t) = V_0(t) - V_1(t), \end{cases} \tag{2}$$

where the dot denotes the derivative with respect to time t. After simple manipulation we obtain the basic systems of equations as follows:

1. *Nonlinear case.*

$$\frac{d^2}{dt^2}\log(1 + V_n(t)) = \begin{cases} V_{n-1}(t) + V_{n+1}(t) - 2V_n(t), & (n \neq 0), \\ V_{-1}(t) + 2V_1(t) - 3V_0(t), & (n = 0). \end{cases} \tag{3}$$

2. *Linear case.*

$$\frac{d^2}{dt^2} V_n(t) = \text{the same as the R.H.S. of (3)} \tag{4}$$

Recall that in the ordinary (non-branched) lattice case, the nonlinear system has a 1-soliton solution such as

$$V_n(t) = \sinh^2 c \, \operatorname{sech}^2(cn - \omega t), \tag{5}$$

where c is a parameter and $\omega = \sinh c$ [12]. This solution represents a pulse wave with amplitude $\sinh^2 c$. On the other hand, the linear equation (4) has a periodic solution

$$V_n(t) = \sin(cn - vt) \tag{6}$$

with low frequency v [12]. Although these facts are well known in the case of the classical lattice, we have no general theory which can be applied to the phenomenon of pulse wave propagation in our branched lattice. Therefore we have to appeal to numerical experiments.

Here we shall describe the numerical experiment in detail only for the linear equation, since the description for the nonlinear equation is similar. In the linear case, the equation to be solved numerically is not the infinite system of equations (4) but the finite system of the differential equations such that

$$\frac{d^2}{dt^2} X(t) = AX(t), \quad 0 \leq t \leq t_f, \tag{7}$$

where $X(t)$ is the $(2N + 1)$-dimensional vector defined by

$$X(t) = (V_{-N}(t), V_{-N+1}(t), \cdots, V_{N-1}(t), V_N(t))^T,$$

and A is the $(2N + 1) \times (2N + 1)$ matrix defined by

$$A = \begin{pmatrix} -2 & 1 & & & & 0 \\ 1 & -2 & 1 & & & \\ & \cdots\cdots & & & & \\ & & 1 & -3 & 2 & \\ & & & \cdots\cdots & & \\ & & & 1 & -2 & 1 \\ 0 & & & & 1 & -2 \end{pmatrix}$$

In our experiment, we take a sufficiently large value of N, say 300, to lessen the effect due to the finiteness of the boundary. Although any of the numerical methods developed so far would be applicable to eq. (7), the Störmer type methods [2], [3] are particularly efficient for the second order equation in which the first derivative of the solution does not appear explicitly as in (7). Here we use Störmer's method of order 3. The recurrence relation of the method is

$$X_{i+3} = 2X_{i+2} - X_{i+1} + \frac{h^2}{12} A(13X_{i+2} - 2X_{i+1} + X_i),$$
$$i = 0, 1, \cdots, I, \quad h = t_f/I, \tag{8}$$

where X_i is a numerical approximation to the solution of (7) at $t = ih$. In solving (7) we start with some relatively large step size h_0, and halve it repeatedly in such a manner that $h = h_0, h_0/2, h_0/4, \cdots$, until the condition

$$\max_v \left| \frac{X_I^{(v)}(h) - X_I^{(v)}(h/2)}{X_I^{(v)}(h/2)} \right| < 10^{-3} \tag{9}$$

is satisfied, where $X_I^{(\nu)}(h)$ is the ν-th element of the numerical solution X_I obtained with the step size h. In (9) the maximum is taken for all ν such that

$$|X_I^{(\nu)}(h)| > \varepsilon,$$

where ε is a small positive value in the range $10^{-8} \sim 10^{-10}$. Throughout the experiments we used the double precision arithmetic of FORTRAN 77, which has a 48-bit mantissa, on the SX-3/44R vector processor at Computer Center of Tohoku University.

2. Conservative quantities

As is well known, the system has three quantities which are physically natural: energy, charge and "momentum". Let us estimate the flows of these quantities through the branch point $n = 0$.

Remark. In this section we shall describe only the case of the nonlinear lattice, for the sake of simplicity of presentation. The linear case can be easily deduced from the approximations

$$\log(1 + V) \simeq V, \quad V - \log(1+V) \simeq \frac{1}{2} V^2 \tag{10}$$

which are valid for small $|V|$.

1. *Energy:* As is well known, in the nonlinear case the electric energy in the n-th capacitor at time t is given by

$$\begin{aligned} U_n(t) &= \int_0^{V_n(t)} V_n \, dQ_n \\ &= \int_0^{V_n(t)} \frac{V_n}{1 + V_n} \, dV_n \\ &= V_n(t) - \log(1+V_n(t)), \end{aligned} \tag{11}$$

and the magnetic energy in the n-th coil is given by

$$T_n(t) = \frac{1}{2} I_n(t)^2. \tag{12}$$

Here let us represent I_n in terms of V_n for convenience of numerical computations. Since we may assume $I_{-\infty} = 0$, we have for $n \leq -1$

$$\begin{aligned} I_n &= -\sum_{k=-\infty}^{n} (I_{k-1} - I_k) \\ &= -\sum_{k=-\infty}^{n} \dot{Q}_k \\ &= -\frac{d}{dt} \sum_{k=-\infty}^{n} \log(1 + V_k), \end{aligned} \tag{13}$$

where (1) and the nonlinear property of Q_k are used. From this we have for $n \leq -1$

$$T_n(t) = \frac{1}{2} \left\{ \frac{d}{dt} \sum_{k=-\infty}^{n} \log(1+V_k(t)) \right\}^2. \tag{14}$$

Now let $E_-(t)$ denote the sum of the energy distributed in the left half lattice ($n \leq -1$) at time $t > 0$. Then we have

$$\begin{aligned} E_-(t) = &\sum_{n=-\infty}^{-1} \{V_n(t) - \log(1 + V_n(t))\} \\ &+ \frac{1}{2} \sum_{n=-\infty}^{-1} \left\{ \frac{d}{dt} \sum_{k=-\infty}^{n} \log(1+V_k(t)) \right\}^2. \end{aligned} \tag{15}$$

Note that $E_0(t)$, the energy at $n = 0$, and $E = E(t)$, the total energy, can also be computed in the same way.

Remark. In later sections, we will consider only the case in which the pulse waves decay exponentially as $n \to \pm \infty$, so there is no difficulty in handling the infinite sums that appeared in (13), (14).

2. *Electric charge:* Let $Q_-(t)$ be the partial sum of the charges stored in the left half lattice at time t. Then we have

$$Q_-(t) = \sum_{n=-\infty}^{-1} \log(1+V_n(t)). \tag{16}$$

Also, let $Q = Q(t)$, the total charge distributed on the whole branched lattice.

3. *"Momentum":* It is known that the momentum of the nonlinear wave in the Toda lattice corresponds to the sum of each current I_n, which is independent of t. Let us state this last fact as a proposition:

Proposition. $I(t) = \sum_{n=-\infty}^{\infty} I_n(t)$ is independent of t.

Proof. It suffices to take the derivative of I. In fact

$$\dot{I} = \sum_{n=-\infty}^{\infty} \dot{I}_n = \sum_{n=-\infty}^{\infty} (V_n - V_{n+1}) = V_{-\infty} - V_{\infty} = 0$$

As before, let $I_-(t)$ denote the "momentum" of the nonlinear wave restricted to the left half lattice:

$$\begin{aligned} I_-(t) &= \sum_{n=-\infty}^{-1} I_n(t) \\ &= -\sum_{n=-\infty}^{-1} \left\{ \frac{d}{dt} \sum_{k=-\infty}^{n} \log (1+V_k(t)) \right\} \\ &= -\frac{d}{dt} \sum_{m=1}^{\infty} m \log (1 + V_{-m}(t)) \end{aligned} \tag{17}$$

3. Linear equation

Hereafter we use another symbol for the solution of (4) in order to distinguish it from that of the nonlinear equations. Let $v_n(t)$ denote the solution of the linear equation (4), and $V_n(t)$ denote that of the nonlinear equation (3).

3.1 *Numerical experiments*

Let us consider the case where the linear equation (4) has the following initial conditions:

$$v_n(0) = \varphi(n) \quad \text{and} \quad \dot{v}_n(0) = \psi(n), \tag{18}$$

where

$$\begin{cases} \varphi(n) = \sinh^2 c \, \operatorname{sech}^2 c(n+p), \\ \psi(n) = 2\varphi(n) \sinh c \tanh c(n+p), \quad (n = 0, \pm 1, \pm 2, \cdots). \end{cases} \tag{19}$$

Note that under the conditions (18) and (19) the Toda lattice yields the 1-soliton solution. In (19), c is a parameter which determines both the amplitude and width of the pulse wave, and p is a positive integer which determines the location of the pulse wave. In our numerical experiments we choose a sufficiently large p such that the pulse wave is located at a position far away from the branching point $n = 0$ at time $t = 0$, i.e., we chose p so that the following conditions are satisfied:

$$v_n(0) \simeq 0, \quad \dot{v}_n(0) \simeq 0, \qquad (n = 0, 1, 2, \cdots) \tag{20}$$

As a consequence, we may expect that $v_n(t)$ has a soliton-like pulse waveform for small t.

In solving differential equation (7) using the numerical method (8) we need three initial values X_0, X_1 and X_2. In our experiments we take the theoretical solutions as these values, that is

$$X_i^{(\nu)} = \sinh^2 c \, \operatorname{sech}^2 (c(\nu + p) - \omega i h), \quad i = 0, 1, 2, \quad \nu = -N, \cdots, N,$$

where $X_i^{(\nu)}$ is the ν-th element of X_i, as before. The graphs of $v_n(t)$ obtained by numerical experiments for $c = 0.1$, 0.3, 0.5 and 1.0 are shown in Fig. 2. Throughout the experiments we have chosen $p = 30$.

Table 1 shows ratios $E_-(t)/E$, $Q_-(t)/Q$ and $I_-(t)/I$ computed numerically using (15), (16), (17) and the approximation (10). In calculating these quantities we used the numerical differentiations

$$\frac{d}{dt} f(t) \simeq \frac{f(t+h) - f(t-h)}{2h},$$

instead of the differentiations appeared in these equations. It follows from the table that the quantities $E_-(t)/E$, $Q_-(t)/Q$ and $I_-(t)/I$ depend on c strongly. In particular, for small c the ratio of energy E_-/E is approximately equal to $(1/3)^2$, but increases considerably as c grows.

3.2 *Observations*

1. In general, the pulse wave $v_n(t)$ is not very stable for large t. For small t, it behaves, however, like a soliton before arriving at the branch point $n = 0$.
2. The behavior of the wave propagation after passing through the point $n = 0$ depends heavily on the value

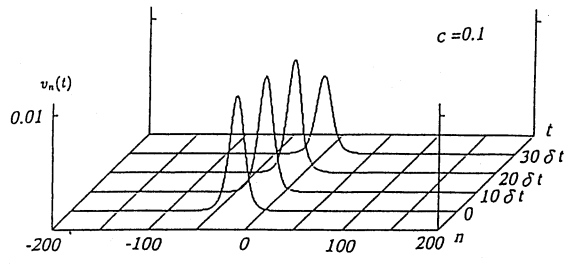

Fig.2-(a)

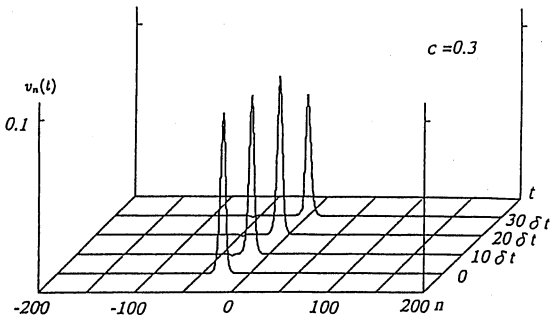

Fig.2-(c)

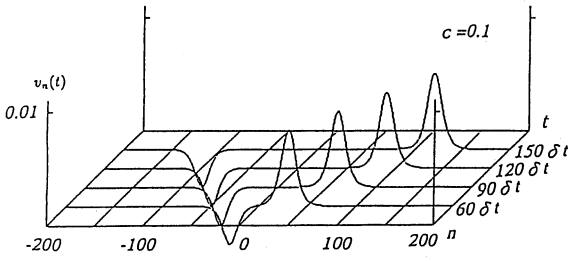

Fig.2-(b)

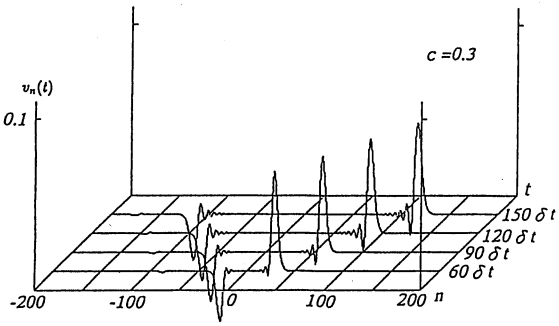

Fig.2-(d)

Linear case

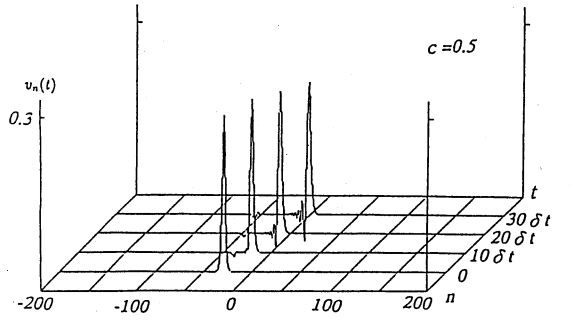

Fig.2.-(e)

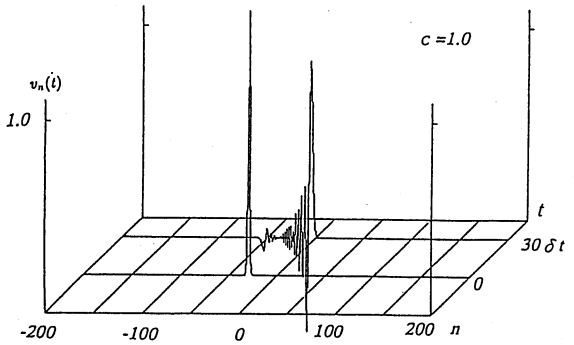

Fig.2-(g)

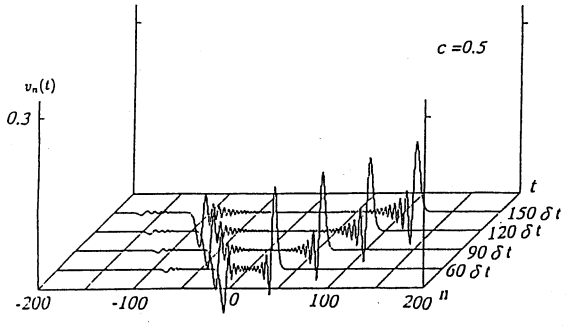

Fig.2(f)

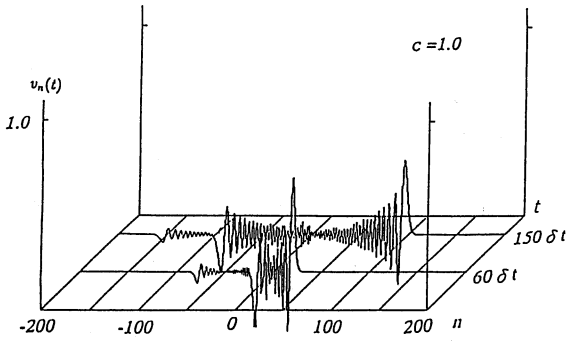

Fig.2(h)

of c. If c is small, the pulse is split smoothly into two stable pulse waves. More precisely, on arriving at $n = 0$, the incident wave changes its form, and subsequently it is transformed into two pulse waves: one is transmitted and the other is reflected with the opposite sign. These pulse waves propagate with the same speed as the incident pulse wave. Moreover, we can observe that the approximate amplitudes of these pulse waves are $2/3$ and $-1/3$ times, respectively, that of the incident pulse wave, respectively.

Table 1.1. Ratios $E_-(t)/E$, $Q_-(t)/Q$ and $I_-(t)/I$ of the linear model for $c=0.1$.

t	$E_-(t)/E$	$Q_-(t)/Q$	$I_-(t)/I$
0	1.00E + 00	9.97E − 01	9.98E − 01
$10\delta t$	9.99E − 01	9.77E − 01	9.85E − 01
$20\delta t$	9.63E + 00	8.40E − 01	9.15E − 01
$30\delta t$	5.50E − 01	3.32E − 01	6.59E − 01
$60\delta t$	1.08E − 01	−3.22E − 01	3.26E − 01
$90\delta t$	1.08E − 01	−3.20E − 01	3.20E − 01
$120\delta t$	1.08E − 01	−3.16E − 01	3.15E − 01
$150\delta t$	1.08E − 01	−3.11E − 01	3.11E − 01

Table 1.2. Ratios $E_-(t)/E$, $Q_-(t)/Q$ and $I_-(t)/I$ of the linear model for $c=0.5$.

t	$E_-(t)/E$	$Q_-(t)/Q$	$I_-(t)/I$
0	1.00E + 00	1.00E + 00	1.00E + 00
$10\delta t$	1.00E + 00	1.00E + 00	1.00E + 00
$20\delta t$	1.00E + 00	1.00E + 00	1.00E + 00
$30\delta t$	8.92E − 01	6.48E − 01	8.36E − 01
$60\delta t$	1.17E − 01	−3.60E − 01	3.48E − 01
$90\delta t$	1.17E − 01	−3.62E − 01	3.47E − 01
$120\delta t$	1.17E − 01	−3.61E − 01	3.47E − 01
$150\delta t$	1.17E − 01	−3.61E − 01	3.47E − 01

Table 1.3. Ratios $E_-(t)/E$, $Q_-(t)/Q$ and $I_-(t)/I$ of the linear model for $c=1.0$.

t	$E_-(t)/E$	$Q_-(t)/Q$	$I_-(t)/I$
0	1.00E + 00	1.00E + 00	1.00E + 00
$10\delta t$	1.00E + 00	9.99E − 01	1.00f + 00
$20\delta t$	1.00E + 00	9.98E − 01	1.00E + 00
$30\delta t$	1.00E + 00	9.85E − 01	9.97E − 01
$60\delta t$	1.71E − 01	−4.52E − 01	3.72E − 01
$90\delta t$	1.53E − 01	−4.48E − 01	3.75E − 01
$120\delta t$	1.50E − 01	−4.42E − 01	3.85E − 01
$150\delta t$	1.50E − 01	−4.43E − 01	3.87E − 01

3. However, if c is not small, for example if $c = 1.0$, then both the transmitted and reflected waves are no longer single pulse waves; they are highly oscillative and travel more slowly than the incident wave.

To explain some facts in the above observations, let us first compare the wave propagation in the branched lattice with that on the corresponding branched network. As a matter of fact, the waveforms of $v_n(t)$ for small c led us to examine a continuous analogue of the wave equation, since the previous values $2/3$ and $-1/3$ have also been found in the solution of the corresponding heat equation in the network case [1].

3.3 *Analytic method for the continuous analogue*

The equation to be considered is the continuous version of the wave equation (4) with suitable initial conditions corresponding to (18). The equation is given by

$$\begin{cases} \dfrac{\partial^2 u}{\partial t^2} = \left(\dfrac{\operatorname{sihn} c}{c}\right)^2 \dfrac{\partial^2 u}{\partial x^2} & (0 < t,\ -\infty < x < \infty), \\ \dfrac{\partial u}{\partial x} = (0_-, t) = 2\dfrac{\partial u}{\partial x} & (0_+, t), \\ u(x, 0) = \varphi(x), \\ \dot{u}(x, 0) = \psi(x), \end{cases} \tag{21}$$

where φ and ψ are the same functions as defined by (19) but with n replaced by the continuous variable x. Now we can state the following theorem, which reconfirms the previous values $2/3$ and $-1/3$, the ratios of the amplitudes of the transmitted and reflected waves to that of the original wave with small c.

Theorem. Let $M = \sinh c/c$. Then, under the preceding conditions, we have

$$u(x, t) = \begin{cases} \dfrac{2}{3}\varphi(x - Mt), & (x > 0), \\ \varphi(x - Mt) - \dfrac{1}{3}\varphi(-x - Mt), & (x < 0). \end{cases}$$

Table 1.4. Ratios $E_-(t)/E$, $Q_-(t)/Q$ and $I_-(t)/I$ of the linear model for $c=3.0$.

t	$E_-(t)/E$	$Q_-(t)/Q$	$I_-(t)/I$
0	6.52E − 00	1.00E + 00	1.00E + 00
$10\delta t$	7.23E − 01	7.52E − 01	1.41E + 00
$20\delta t$	7.23E − 01	5.03E − 01	1.41E + 00
$30\delta t$	7.23E − 01	2.55E − 01	1.41E + 00
$60\delta t$	7.23E − 01	−4.91E − 01	1.41E + 00
$90\delta t$	7.22E − 01	−1.26E + 00	1.40E + 00
$120\delta t$	5.43E − 01	−2.46E + 00	1.30E + 00
$150\delta t$	4.86E − 01	−2.79E + 00	1.39E + 00

Outline of the Proof. Details are omitted for convenience of the presentation (see [1]). By the conventional technique of separation of variables, the problem is reduced to construct first the Green function $G = G(x, y, \lambda)$, which satisfies

$$\begin{cases} \dfrac{d^2G}{dx^2} = \lambda G, \quad (x \neq y) \\ \dfrac{dG}{dx}(0_-, y, \lambda) = 2\dfrac{dG}{dx}(0_+, y, \lambda), \\ \dfrac{dG}{dx}(y-0, y, \lambda) - \dfrac{dG}{dx}(y+0, y, \lambda) = 1. \end{cases} \tag{22}$$

Then, for $y < 0$, G is given by

$$G(x, y, \lambda) = \begin{cases} \dfrac{e^{\sqrt{\lambda}(y-x)}}{3\sqrt{\lambda}}, & (x > 0), \\ \dfrac{1}{2\sqrt{\lambda}}\left(e^{\sqrt{\lambda}(y-x)} - \dfrac{e^{\sqrt{\lambda}(y+x)}}{3}\right), & (x < 0). \end{cases} \tag{23}$$

Secondly, we represent the solution u in terms of φ and ψ. Using the complex integral we have

$$u(x, t) = \frac{1}{2\pi i}\int_\Gamma \int_{-\infty}^{\infty} G(x, y, \lambda)\, dy d\lambda \times \left(\cosh(M\sqrt{\lambda}\, t)\varphi(y) + \frac{\sinh(M\sqrt{\lambda}\, t)}{M\sqrt{\lambda}}\psi(y)\right), \tag{24}$$

where Γ is a path around the negative real axis. Then, finally, it suffices to apply the integration by parts taking into account the following equalities

$$\psi(y) = -M\frac{d\varphi(y)}{dy}, \tag{25}$$

$$\frac{1}{2\pi i}\int_\Gamma \frac{e^{\sqrt{\lambda}z}}{2\sqrt{\lambda}} d\lambda = \delta(z). \tag{26}$$

∎

Now, let us continue our explanation of the preceding observations. First of all, it is natural that, in general, $v_n(t)$ changes its waveform to some extent even before coming close to the branch point $n = 0$ because the 1-soliton is not an exact solution of the linear equation. Secondly, if c is small, which implies that the amplitude of $v_n(t)$ is small, then $v_n(t)$ preserves its waveform, since the nonlinear equation does not differ so much from the linear equation for small amplitude. Furthermore, if c is small, the collision of the pulse wave at $n = 0$ is described very well by that of the continuous analogue. Nevertheless, for larger values of c, the situation changes remarkably. In fact, when $c = 1$, we can observe a different phenomenon: the scattered waves are highly oscillative and are very different from those of the case $c = 0.1$. The reason may be that, if c is not small, an incident pulse with high "frequency" excites a disturbance of high frequency $\simeq \omega(= \sinh c)$ in the vicinity of $n = 0$, which is considerably larger than $2 \sin |c/2|$, the cut off frequency of the dispersion relation for sine periodic waves in the linear lattice [12]. Consequently, together with the theorem, our observations emphasize again the difference between our discrete model and its continuous analogue in the case where c is not small. The cut off frequency is also related to the following localized oscillation.

3.4 *Localized mode*

Let us discuss the existence of a localized oscillation which may possibly be excited in the vicinity of the

branching point. For this purpose we introduce a generalized model of our linear branched LC network where the value of the capacitance of the 0-th capacitor is replaced by k (as before, the values of other capacitors are normalized to unity). Then the circuit equation of this model is given by

$$\frac{d^2}{dt^2} V_n(t) = \begin{cases} V_{n-1}(t) + V_{n+1}(t) - 2V_n(t), & (n \neq 0), \\ \dfrac{1}{k}(V_{-1}(t) + 2V_1(t) - 3V_0(t)), & (n = 0). \end{cases} \tag{27}$$

Let us assume that there exists a localized mode of the form

$$V_n(t) = a^{|n|} \sin bt, \quad (n = 0, \pm 1, \pm 2, \cdots), \tag{28}$$

where a and b are real constants. Then a simple computation shows that the system of equations (27) has the solution (28) with $a = k/(k-3)$, $b = 3/\sqrt{k(3-k)}$. Also $|a| < 1$, if and only if $0 < k < 3/2$. Note that $k = 3/2$ corresponds to $a = -1$ and $b = 2$ which is the preceding cut off frequency ($c = \pi$ in the defining formula). In [13] this kind of localized mode has already been discussed in another situation of the dynamic model which contains a light mass impurity at $n = 0$. This equation is, however, different from ours around $n = 0$. In Sec. 4 we shall depict the graphs of the linear oscillation $v_0(t)$ and the nonlinear oscillation $V_0(t)$ obtained by numerical experiments. In this respect, it is noteworthy that, in the vicinity of $n = 0$, we find no localized mode in our numerical solutions for small c, although this mode is theoretically allowed to exist since $k = 1$ in our experiment.

Finally we note that the localized mode comes from the L^2 point spectrum for the second order difference operator defined in the branched lattice.

4. Nonlinear equation

4.1 *Numerical experiments*

Let $V_n(t)$ be the solution of the nonlinear equation (3) with the same initial conditions as those of $v_n(t)$. That is, the initial values of the equation (3) are defined by (18) and (19). Then $V_n(t)$ is expected to be a pulse wave close to a 1-soliton until it reaches to $n = 0$. We have computed $V_n(t)$ and the ratios concerning the conservative quantities numerically for various c.

In Table 2 the ratios $E_-(t)/E$, $Q_-(t)/Q$, and $I_-(t)/I$ are shown for various t, where $\delta t = c/\omega$. Again, we can observe that these quantities depend on c. Remarkable differences between the results in Table 1 and those in Table 2 are already apparent when $c = 1$.

4.2 *Observations*

1. If c is very small, for example $c = 0.1$, then the nonlinear pulse wave behaves as if it were a linear wave. The incident 1-soliton is split into a transmitted and a reflected pulse wave; the ratios of the amplitudes of these waves to that of the incident wave are $2/3$ and $-1/3$, as before. These two waves travel with the same speed as the incident pulse wave, and seem to be surprisingly stable, although they are not really 1-solitons since neither the ratios *speed/magnitude* nor *width/magnitude* satisfy the required conditions for 1-solitons.
2. If c is relatively small, $c = 0.5$ for example, then just after passing through the branch point $n = 0$, the waveforms are still rather close to those computed theoretically in the continuous model. In fact, the speeds and widths of the transmitted and reflected pulse waves are almost the same as the incident pulse wave. We may even say that the resulting pulse waves are considerably more stable in the nonlinear case than in the linear case. But as the two pulse waves continue to propagate, their magnitudes decrease slightly, and the oscillations appear and grow gradually in the trailing edge of both pulses. This description is particularly pertinent to the reflected wave. Its magnitude decreases in a steady way and its traveling speed slows down slightly. Also, another remarkable fact is that a localized mode is excited in the vicinity of $n = 0$, contrary to the linear case.
3. As the value of c increases, the phenomena become more complex. Let us see what happens when $c = 1.0$. First, the oscillating wave accompanying the reflected pulse wave becomes significant and is observed in the whole part of the left half lattice. We may say that the reflected wave is transformed into a traveling oscillation. Secondly, it is remarkable that the transmitted pulse wave preserves almost the same waveform, amplitude and speed for a large time. When c is larger, for example $c = 3.0$, then even the transmitted wave is no longer a single pulse wave. Two pulses appear and they carry a large part of the whole energy! This is an interesting unexpected phenomenon due to a strong nonlinear effect and merits further investigation.

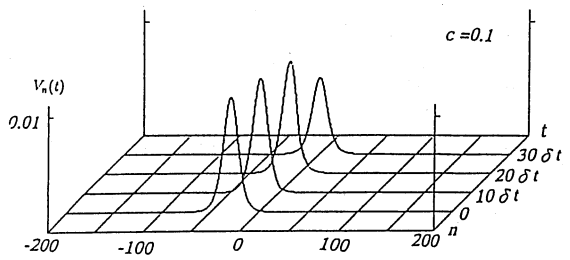

Fig.3-(a)

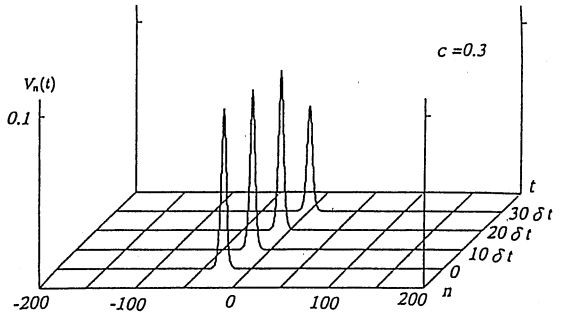

Fig3.-(c)

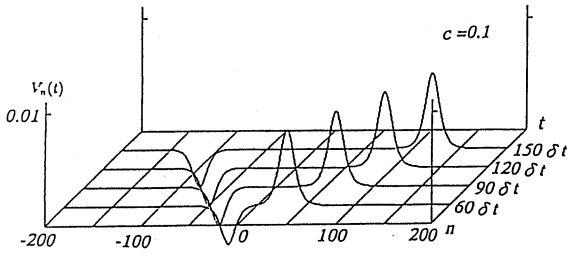

Fig.3-(b)

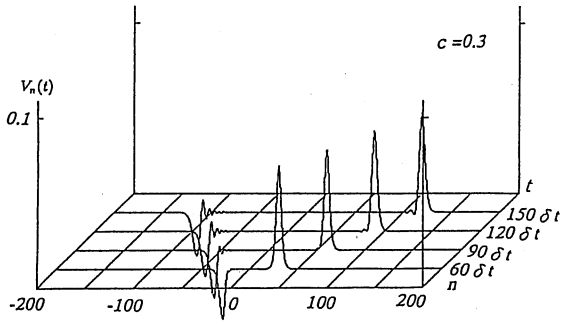

Fig.3-(d)

Nonlinear case

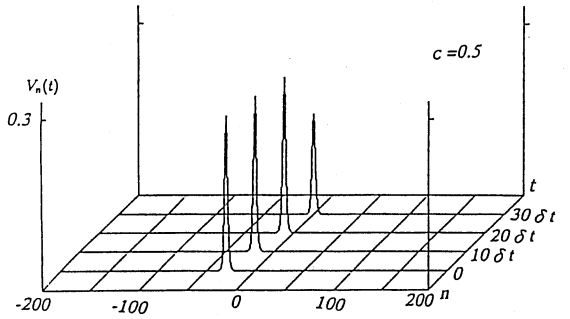

Fig.3-(e)

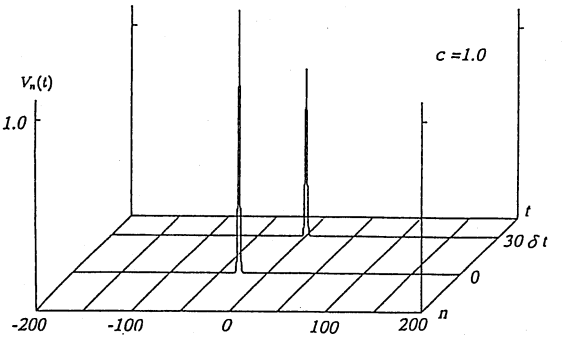

Fig.3-(g)

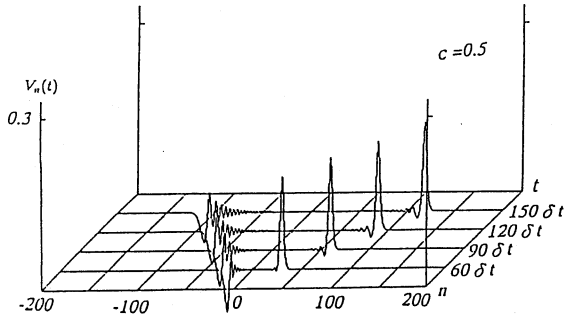

Fig.3-(f)

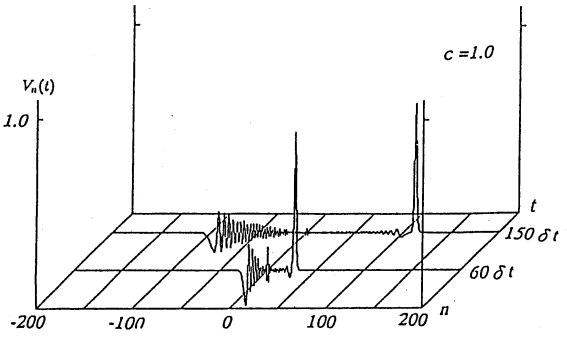

Fig.3-(h)

4.3 *Graphs of localized modes*

The excitation of a localized mode has been discussed in the linear case in Sec. 3. A localized mode is allowed when $0 < k < 3/2$. On the other hand, the localized mode in the nonlinear lattice is not easy to analyze theoretically because of the nonlinearity for a particularly large c. The following are the graphs of the solutions $v_0(t)$ and $V_0(t)$ at the branch point $n = 0$. Here we have fixed $k = 1$.

Table 2.1. Ratios $E_-(t)/E$, $Q_-(t)/Q$ and $I_-(t)/I$ of the nonlinear model for c=0.1.

t	$E_-(t)/E$	$Q_-(t)/Q$	$I_-(t)/I$
0	1.00E + 00	9.97E − 01	9.98E − 01
$10\delta t$	9.99E − 01	9.77E − 01	9.85E − 01
$20\delta t$	9.63E + 00	8.39E − 01	9.14E − 01
$30\delta t$	5.44E − 01	3.28E − 01	6.56E − 01
$60\delta t$	1.08E − 01	−3.21E − 01	3.25E − 01
$90\delta t$	1.08E − 01	−3.20E − 01	3.19E − 01
$120\delta t$	1.08E − 01	−3.15E − 01	3.15E − 01
$150\delta t$	1.08E − 01	−3.11E − 01	3.10E − 01

Table 2.2. Ratios $E_-(t)/E$, $Q_-(t)/Q$ and $I_-(t)/I$ of the nonlinear model for c=0.5.

t	$E_-(t)/E$	$Q_-(t)/Q$	$I_-(t)/I$
0	1.00E + 00	1.00E + 00	1.00E + 00
$10\delta t$	1.00E + 00	1.00E + 00	1.00E + 00
$20\delta t$	1.00E + 00	1.00E + 00	1.00E + 00
$30\delta t$	5.13E − 01	2.82E − 01	6.45E − 01
$60\delta t$	1.16E − 01	−3.53E − 01	3.33E − 01
$90\delta t$	1.16E − 01	−3.53E − 01	3.33E − 01
$120\delta t$	1.16E − 01	−3.51E − 01	3.33E − 01
$150\delta t$	1.16E − 01	−3.53E − 01	3.34E − 01

Table 2.3. Ratios $E_-(t)/E$, $Q_-(t)/Q$ and $I_-(t)/I$ of the nonlinear model for c=1.0.

0	1.00E + 00	1.00E + 00	1.00E + 00
$10\delta t$	1.00E + 00	1.00E + 00	1.00E + 00
$20\delta t$	1.00E + 00	1.00E + 00	1.00E + 00
$30\delta t$	4.67E − 01	2.32E − 01	6.25E − 01
$60\delta t$	1.21E − 01	−4.33E − 01	3.37E − 01
$90\delta t$	1.22E − 01	−3.95E − 01	3.36E − 01
$120\delta t$	1.22E − 01	−4.23E − 01	3.06E − 01
$150\delta t$	1.23E − 01	−4.18E − 01	3.52E − 01

Table 2.4. Ratios $E_-(t)/E$, $Q_-(t)/Q$ and $I_-(t)/I$ of the nonlinear model for c=3.0.

0	1.00E + 00	1.00E + 00	1.00E + 00
$10\delta t$	1.00E + 00	1.00E + 00	1.00E + 00
$20\delta t$	1.00E + 00	1.00E + 00	1.00E + 00
$30\delta t$	3.72E − 01	1.01E − 01	6.04E − 01
$60\delta t$	2.97E − 02	−9.57E − 01	1.94E − 01
$90\delta t$	2.71E − 02	−9.12E − 01	1.74E − 01
$120\delta t$	2.75E − 02	−9.50E − 01	1.64E − 01
$150\delta t$	2.72E − 02	−9.98E − 01	1.70E − 01

They show the following:

1. *For* $c = 0.1$, there is no oscillation in the vicinity of $n = 0$ for both linear and nonlinear cases.
2. *For* $c = 0.5$, a localized mode is excited at $n = 0$, but its amplitude decays rapidly with time in the linear case, whereas a small localized mode seems to last for a long time in the nonlinear case. They are different modes because their frequencies differ from each other.
3. *For* $c = 1.0$, a localized mode is strongly excited, but it diminishes steadily with time in the linear case. In the nonlinear case, we can observe a regular oscillation at $n = 0$. These graphs show that the numerical results agree well with the widely accepted theory that the dynamics in the linear lattice don't have an ergodic property, whereas the dynamics in the nonlinear lattice do [8], [9], [14].

5. Discussion

We have investigated numerically the phenomenon of linear and nonlinear wave propagations in a branched lattice. The required condition for a solution of the wave equation is naturally deduced from the introduction of the branched infinite LC circuit model. We have performed numerical experiments of the scattering of incident pulse waves at the branch point $n = 0$. As the incident pulse waves, we used a family of lattice solitons in the nonlinear case and soliton-like pulse waves in the linear case. In the linear case it would be possible to determine

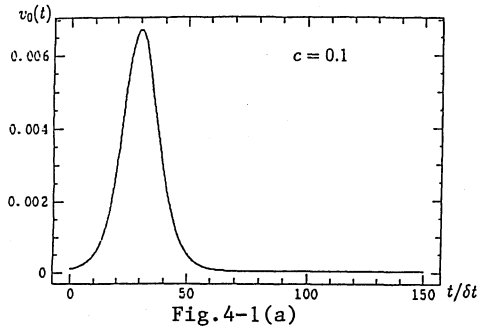

Fig.4-1(a)

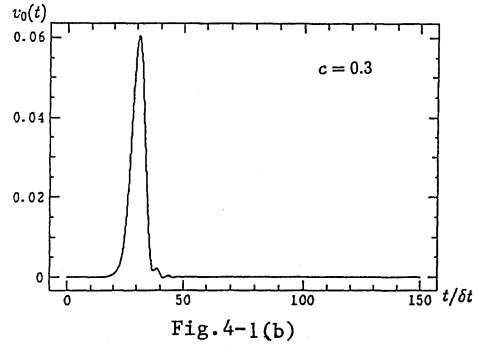

Fig.4-1(b)

Linear

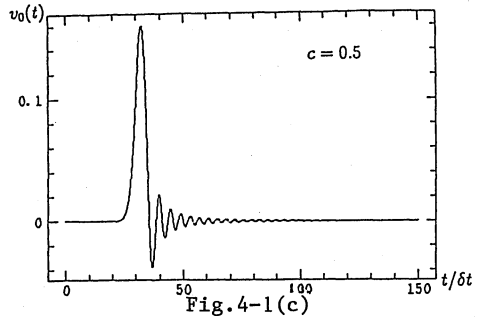

Fig.4-1(c)

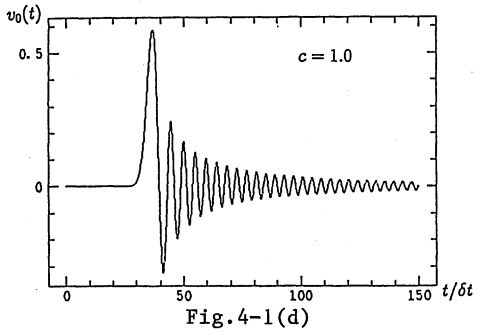

Fig.4-1(d)

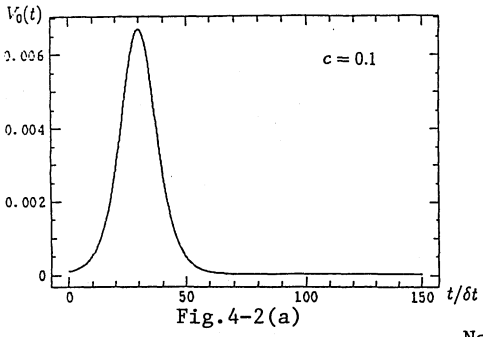

Fig.4-2(a)

Nonlinear

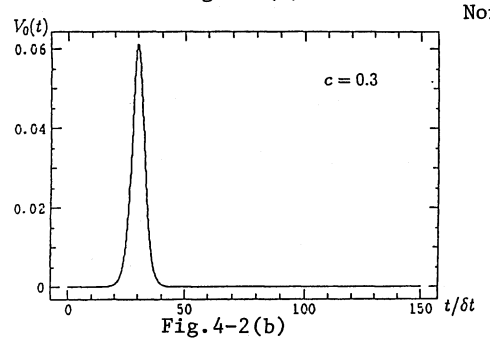

Fig.4-2(b)

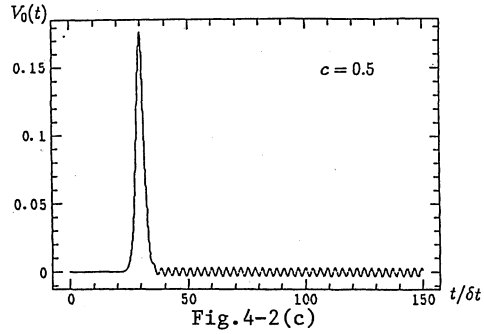

Fig.4-2(c)

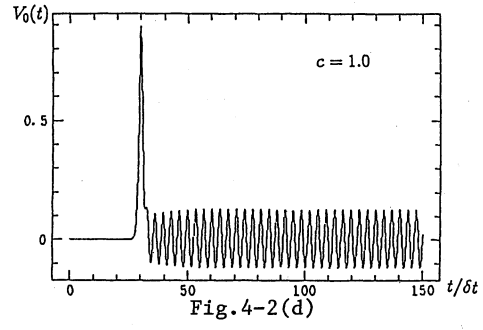

Fig.4-2(d)

the solution of the wave equation analytically by computing a lattice Green function, as in Sec. 3, but this approach may not be practical.

Here we shall review our results:

1. *On the scattered wave.* First of all, we can find from the numerical experiments that, if the amplitudes of the incident waves are small, then the solutions of the nonlinear equation are approximately the same as those of the corresponding linear equation, as is expected in almost all physical phenomena. We have also found that the scattered waves, consisting of a transmitted and a reflected pulse wave behave similarly in both the linear and nonlinear cases if the amplitude of the incident wave is small. Secondly, the waveforms of the solutions in both cases agree well with those of solutions of the continuous analogue, which were computed by an analytic method. However, if the amplitude of the incident pulse is not small, this is no longer valid, namely, scattered waves in the branched lattice (i.e. a discrete model) have considerably different shapes from those in the branched network (i.e. a continuous model). More precisely, the former does not consist of clear pulse waves any more. In fact, according to the numerical experiments, the reflected wave is accompanied by oscillating waves in its trailing edge, and it gradually

loses speed and decreases in amplitude, as it travels away from the branch point. This is a common feature of linear and nonlinear waves with moderate amplitudes. On the other hand, there also arises a remarkable difference between linear and nonlinear waves concerning the transmitted waves if the wave amplitude is not small. In the nonlinear case, the transmitted wave tends to preserve its pulse-like waveform. Consider the case $c = 1.0$, for example, then the transmitted nonlinear pulse wave seems to be rather stable for a long time after passing through the branch point. Furthermore, a surprising phenomenon occurs if c becomes larger: when $c = 3.0$, for example, we have observed two transmitted pulse waves which may be produced by the effect of the strong nonlinearity.

2. *On the conservative quantities.* In Sections 3 and 4 we have given tables of ratios of the physical quantities. The values in these tables do not depend so much on time for large t, as long as c is small. Also, for small c, there is not much difference between the linear and nonlinear cases. On the other hand, as c increases, the reflected energy increases rapidly in the linear case, whereas it tends to decrease in the nonlinear case. The data for $c = 3.0$ are somewhat surprising. This result, however, is probably not so accurate because of the discretization and/or roundoff error during computation: note that both the amplitude and slope of the solution are surprisingly large. Further investigation will be necessary to reach a definitive conclusion about the scattering of incident pulses with large parameter c.
3. *On the localized modes.* From the numerical experiments in both the linear and nonlinear cases for small c, we cannot find any localized mode in the vicinity of the branching point. However, the localized mode is excited in the nonlinear case if c is not very small, for example $c = 0.5$. In general, we may expect that the larger the value of c, the larger the amplitude of the localized mode. On the contrary, we have not found any stable local mode excited in the vicinity of $n = 0$ in the linear case, although, as is seen in Sec. 3, its existence is allowed theoretically. In fact, the disturbance at $n = 0$ caused by the incident pulse wave generates an oscillation but its amplitude decays gradually with the time. These contrasting phenomena may be related to the so called ergodic (recurrent) property of the nonlinear (linear) lattice.

Further investigations will be necessary for a full understanding of these phenomena.

Acknowledgment

The second author is grateful to Professor H. Kawakami of Tokushima University for stimulating discussions concerning electric circuits.

REFERENCES

[1] Gaveau, B., Okada, T. and Okada, M., (1993), Explicit heat kernels on graphs and spectral analysis, Mathematical Notes 38, Princeton Univ. Press: 364–388.
[2] Hairer, E., Nørsett, S. P. and Wanner, G., (1987), Solving Ordinary Differential Equations I (Nonstiff Problems), Springer-Verlag, Berlin.
[3] Henrici, P., (1962), Discrete Variable Methods in Ordinary Differential Equations, John Wiley & Sons, New-York.
[4] Hirota, R. and Suzuki, K., (1970), Studies on lattice by using electrical networks, J. Phys, Soc, Jpn. 28: 1366–1367.
[5] Kametaka, Y., (1977), Nonlinear Partial Differential Equation (in Japanese), Sangyou-Tosyo, Tokyo.
[6] Lax, P. D., (1968), Integrals of evolution and solitary waves, Communications on Pure and Applied Mathematics 21: 467–490.
[7] Mimura, M. and Satsuma, J., (1985), Ecotons ofa nonlinear diffusion equation, RIMS Kokyuroku 554, Kyoto Univ.: 184–199.
[8] Payton III, D. N., Rich, M. and Visscher, W. M., (1967), Lattice thermal conductivity in disordered harmonic and anharmonic crystal models, Phys. Rev. 160: 706–711.
[9] Saito, N., Ooyama, N., Aizawa, Y. and Hirooka, H., (1970), Computer experiments on ergodic problems in anharmonic lattice vibrations, Prog. Theor. Phys. Suppl. 45: 209–230.
[10] Scott, A. C., Chu, F. Y. F. and McLaughlin, D. W., (1973), The soliton: A new concept in applied science, Proc. IEEE 61: 1443–1483.
[11] Toda, M., (1967), Wave propagation in anharmonic lattices, J. Phys. Soc. Jpn. 23: 501–506.
[12] Toda, M., (1981), Theory of Nonlinear Lattices, Springer, Berlin.
[13] Watanabe, S. and Toda, M., (1981), Interaction of soliton with an impurity in non-linear lattice, J. Phys. Soc. Jpn. 50: 3436–3442.
[14] Zabusky, N. J. and Kruskal, M. D., (1965), Interaction of solutions in a collisionless plasma and the recurrence of initial states, Phys. Rev. Lett. 15: 240–243.